# EXAFS study of PbS–SnS solid solution

## Alexander Lebedev, Irina Sluchinskaya and Ian Munro

# EXAFS study of PbS–SnS solid solution

**Alexander Lebedev,**[a]* **Irina Sluchinskaya**[a] **and Ian Munro**[b]

[a]*Physics Department, Moscow State University, Moscow 119899, Russia, and* [b]*CLRC Daresbury Laboratory, Warrington, WA4 4AD, UK. E-mail: swan@mch.chem.msu.su*

The local environment of the Pb atom in $Pb_xSn_{1-x}S$ solid solution was studied by EXAFS technique. The shortest Pb–S bond length in orthorhombic samples was found to be by $\approx 0.2$ Å shorter than in cubic PbS. This indicates that the $6s^2$ lone pair of Pb is stereochemically active in the SnS host. Strong correlations found in the distribution of metal atoms in the second shell show that the orthorhombic samples can be considered as solid solutions with unexpectedly strong short-range order. One can expect that the short-range order in $PbSnS_2$ may result in formation of superstructures with space groups $C_{2v}^7$ or $C_{2v}^2$.

## 1. Introduction

Semiconductor solid solutions with a layered structure have attracted considerable attention due to their possible application in optoelectronics.

First investigations of the PbS–SnS system (Morozov *et al.*, 1963; Kuznetsov *et al.*, 1964; von Krebs *et al.*, 1964) have established a rather complex constitution of its phase diagram resulting from different crystal structures of SnS and PbS. SnS has an orthorhombic structure (space group $D_{2h}^{16}$) and consists of double layers weakly bound to each other while PbS has a cubic NaCl structure (space group $O_h^5$). The solubility of SnS in PbS is limited by $\approx 10$ mol.% while that of PbS in SnS is about 50 mol.%. Despite many experiments done on the system, there is still a divergence of opinions concerning the structure of the $PbSnS_2$ composition in this system. Some authors believe that this composition is an individual phase and has the same space group as SnS (Kuznetsov *et al.*, 1964; Baak *et al.*, 1966; Bigvava *et al.*, 1974) or a different ($D_{2h}^{13}$ or $C_{2v}^7$) space group (Kuznetsov *et al.*, 1964; Bigvava *et al.*, 1974). Other authors believe that this composition belongs to SnS-based solid solution (Morozov *et al.*, 1963; von Krebs *et al.*, 1964; Latypov *et al.*, 1976; Nuriev *et al.*, 1986). So, one of the purposes of our investigation was to study the local structure of Pb in $PbSnS_2$ samples in order to clarify this discrepancy.

Another cause of our interest to the PbS–SnS system is associated with the off-centering of large (Pb, Sn) impurity atoms in GeTe recently observed by Lebedev *et al.* (1997). This effect was explained by the participation of the $s^2$ lone pair of impurity in chemical bonding. This was very unexpected for the Pb as in compounds of divalent lead its $6s^2$ lone pair is usually inactive, and the local environment of Pb is symmetric (like in PbS). So, the other purpose of our work was to study if the $6s^2$ lone pair of Pb becomes stereochemically active when entering SnS.

## 2. Sample preparation and data analysis

Samples of $Pb_xSn_{1-x}S$ solid solutions ($x = 0.1, 0.2, 0.35, 0.5, 0.95$) were prepared by alloying PbS and SnS in evacuated silica ampoules and were annealed at $645°C$ for 70–96 h. X-ray studies confirmed the homogeneity of the samples and showed that they had the orthorhombic structure at $x \leq 0.5$ and the cubic structure at $x \geq 0.95$. Before EXAFS measurements the samples were powdered, sieved and the powder was rubbed into the surface of adhesive tape. The optimal thickness of absorbing layer was obtained by folding the tape.

EXAFS experiments were carried out on station 7.1 of the Daresbury SRS at an electron beam energy of 2 GeV and a maximum stored current of 230 mA in transmission mode. The beam was monochromatized using two Si(111) crystal monochromator; the intensities of incident and transmitted beams were registered using ion chambers. Measurement were made at 80 K at the Pb $L_{III}$ edge (13.055 keV). For each sample two independent measurements were made.

The extraction of EXAFS $\chi(k)$ function from the absorption spectra $\mu x(E)$ were made as in the previous work (Lebedev *et al.*, 1997). After removal the pre-edge background, splines were used to extract the smooth atomic part of absorption, $\mu x_0(E)$, and then the dependence $\chi = (\mu x - \mu x_0)/\mu x_0$ was calculated as a function of the photoelectron wave vector $k = \sqrt{2m(E - E_0)}/\hbar$. The energy origin, $E_0$, was taken as the energy corresponding to the inflection point on the absorption edge. The edge steps varied from 0.1 to 1.5.

Direct and inverse Fourier transforms with modified Hanning windows were used to extract the information about three nearest shells from the $\chi(k)$ curves. Typical range of extraction in $R$-space was 1.2–3.7 Å. The distances $R_j$, coordination numbers $N_j$, and Debye-Waller factors $\sigma_j^2$ for each of three shells ($j = 1$–3) were obtained by minimizing the root-mean-square deviation between the experimental and calculated $k^2\chi(k)$ curves. Along with the structural parameters, the energy origin correction $dE_0$ was varied simultaneously. To decrease the number of fitting parameters, known relations between the coordination numbers for known structures were taken into account. The number of fitting parameters (8) was about half of the number of independent data points ($2\Delta R\Delta k/\pi = 15$–16). The accuracy in the parameters determination was estimated from the covariance matrix and corresponded to a 95% confidence level interval.

The backscattering amplitude and phase as well as the central-atom phase shift and the mean free path of a photoelectron, which were necessary to calculate theoretical $\chi(k)$ curves, were calculated using FEFF software (Mustre de Leon *et al.*, 1991).

## 3. Results

Typical $k^2\chi(k)$ curves for $Pb_xSn_{1-x}S$ samples are presented in Figure 1. It is seen that the curves for cubic ($x \geq 0.95$) and orthorhombic ($x \leq 0.5$) samples differ qualitatively, thus indicating different local environment of Pb atoms in them. The data analysis revealed that in PbS and $Pb_{0.95}Sn_{0.05}S$ the Pb is surrounded by 6 S atoms at equal distance $R_1$ (see Table 1). For orthorhombic samples the spectra can be described well only in the model, in which the first shell of Pb consists of two subshells: 3 S atoms at one distance $R_1$ and 3 other S atoms at another distance $R_2$ (see Table 1). When increasing $x$ from 0.1 to 0.5 the distance $R_1$ remains unchanged within the experimental error, and the distance $R_2$ decreases a little (see Table 1 and Figure 2). An attention should be paid on high enough values of Debye-Waller (DW) factor for the longer Pb–S bond ($\sigma_2^2$).

The metal (Pb, Sn) atoms in the second shell in orthorhombic samples are at a mean distance of $R_3 \approx 3.5$ Å. DW factors for this shell ($\sigma_3^2$) increase appreciably with increasing $x$.
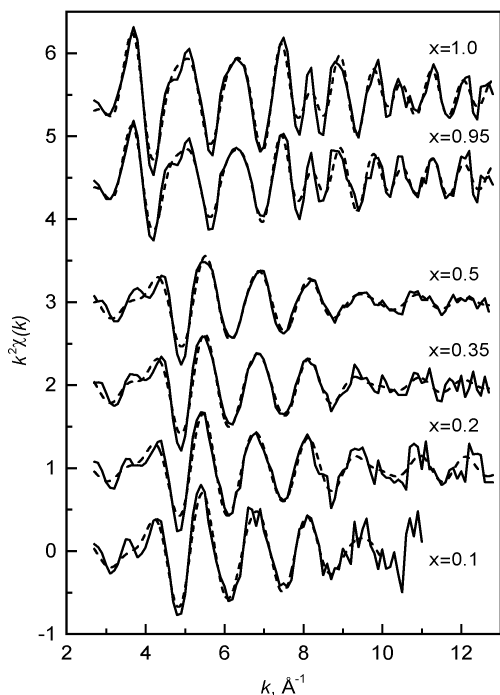
## Figure 1

Experimental $k^2\chi(k)$ spectra obtained at the Pb $L_{III}$ edge for $Pb_xSn_{1-x}S$ samples (solid lines) and their best theoretical approximation (dashed lines).
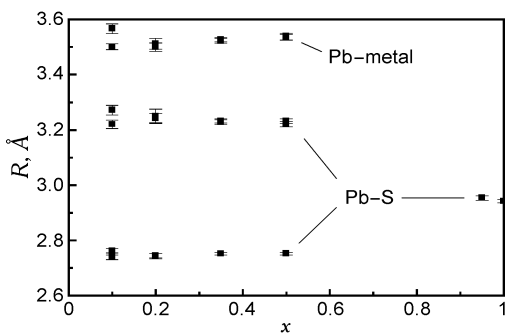
## Figure 2

The composition dependence of interatomic distances to three nearest shells about the Pb atom in $Pb_xSn_{1-x}S$.

As follows from Table 1, in orthorhombic samples the highest values of Debye-Waller factor are those for the longer Pb–S bond, and they do not depend much on composition. The study of the temperature dependence of DW factors in $Pb_{0.8}Sn_{0.2}S$ in the 77–300 K temperature range showed that the variation of $\sigma_2^2$ with temperature was the largest. So, we conclude that high DW factor and its strong temperature dependence for the longer Pb–S bond indicate the weakness of this bond.

As the individual properties of Sn and Pb atoms are different, we could not exclude the existence of the short-range order in the distribution of metal atoms. To check this possibility we compared experimental EXAFS spectra with theoretical ones calculated for different local concentrations of Sn atoms in the second shell of Pb assuming that the distances and DW factors for Pb and Sn are

equal. As follows from Figure 3, for the samples with $x = 0.2$, 0.35, and 0.5 the deviation between experimental and calculated curves is minimal when the short-range order is taken into account, and the local Sn concentration in the second shell of Pb is close to 100%. The appearance of such a short-range order, where Pb atoms are predominantly surrounded by Sn, can be explained by the deformation interaction of the metal atoms, due to which the neighborhood of two large Pb atoms is energetically unfavorable.
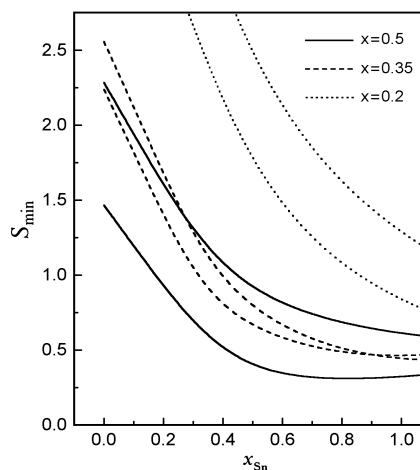
## Figure 3

The sum of the squares of the residuals as a function of local concentration of Sn atoms in the second shell of Pb. Different curves correspond to different spectra obtained for the same sample.

## 4. Discussion

According to the structural data obtained from the neutron diffraction (Chattopadyay *et al.*, 1986), six S atoms in the first shell of Sn in SnS are located at four different distances (1 atom at 2.627 Å, 2 atoms at 2.665 Å, 2 atoms at 3.290 Å, and 1 atom at 3.388 Å). Two shortest distances are so close that EXAFS analysis cannot resolve them. The same is true for two longest distances. Therefore, the nearest environment of the metal atom in the structure is presented in EXAFS spectra by one short and one long averaged distances. The shorter Pb–S bond length obtained from EXAFS data for orthorhombic samples of $Pb_xSn_{1-x}S$ appeared to be by $\approx 0.1$ Å longer than the corresponding averaged Sn–S bond length in SnS, and the longer Pb–S bond length was by $\approx 0.08$ Å less than the corresponding averaged Sn–S bond length in SnS.

The most important fact in these data is that the shorter Pb–S bond in orthorhombic samples is notably (by $\approx 0.2$ Å) less than the Pb–S bond in cubic PbS. It is interesting to note that the contraction of the Pb–S bond length in orthorhombic SnS compared to cubic PbS is close to that observed for the Pb–Te bond in rhombohedral GeTe compared to cubic PbTe (Lebedev *et al.*, 1997). In the same time, no distortion of the Pb environment was observed by us in cubic SnTe doped with Pb. So, we can see that the local distortion of the Pb environment occurs only when impurity Pb atom enters the host, the symmetry of which is lower than cubic. We attribute the observed distortion in $Pb_xSn_{1-x}S$ to the activation of the $6s^2$ lone pair of Pb. We think that this lone pair, which is inactive in lead chalcogenides, remains quite movable and can easily transform into an active state under some circumstances. This peculiarity of the lone pair can be the cause of structural instability and

phase transitions, which are characteristic for many compounds of divalent Pb.

Our results showing that all distances in the local environment of Pb in orthorhombic samples of $Pb_xSn_{1-x}S$ change monotonously with $x$ and there is a strong correlation in the distribution of metal atoms give evidence that the composition $PbSnS_2$ in the PbS–SnS system should be treated as a solid solution with unexpectedly strong short-range order.

The existence of the short-range order, for which Pb atoms in one double layer have as neighbors Sn atoms in the adjacent double layer (see Figure 4($a$)), enables to suppose that in proper conditions a superstructure ordering of the metal atoms can occur in $PbSnS_2$. We guess that such an ordering can be found in geological samples of teallite.

Assuming that the local concentration of Sn in the second shell of Pb is exactly 100%, one can expect the appearance of a completely ordered arrangement of the metal atoms in adjacent double layers of $PbSnS_2$. This ordering will be manifested as zigzag chains ...–Pb–Sn–Pb–Sn–... going along the $c$ axis (perpendicular to the plane of Figure 4($a$)). However, even if the atoms in one chain are completely ordered, the 3-dimensional long-range order can occur only if the arrangement of the atoms in adjacent chains is correlated.

It should be noted that the appearance of zigzag chains results in disappearance of the inversion center in a crystal. This means that the space group of a superstructure should be a subgroup of $D_{2h}^{16}$ and should belong to the $C_{2v}$ point group. If we restrict our consideration by superstructures that do not change the unit cell volume, there are two possible ways to order the metal atoms in the superstructure: one, for which the double layer contains two like atoms (space group $C_{2v}^7$ — $P2_1nm$, see Figure 4($b$)), and the other, for which every double layer contains both types of metal atoms (space group $C_{2v}^2$ — $Pb2_1m$, see Figure 4($c$)). In the former superstructure the ($00l$) reflections with odd $l$ are allowed, and in the latter superstructure the ($00l$) and ($l00$) reflections with odd $l$ are allowed.

A few extra reflections characteristic for the $C_{2v}^2$ superstructure were observed by electron diffraction on thin films of $PbSnS_2$ evaporated onto the alkali halide substrates at $200°$C (Latypov *et al.*, 1976). To reproduce this result, we annealed the sample of $PbSnS_2$ at $240°$C for one month. Unfortunately, the x-ray study of annealed sample did not found any indication of superstructure reflections. We think that the energy of interaction of chains, the closest distance between which is $\approx$4.1 Å, is too low, and the sample needs to be annealed at lower temperature. Therefore, the peculiarity of the PbS–SnS system is that the *interlayer* interaction of the metal atoms is much stronger than the *intralayer* interaction; this is possibly due to different interatomic distances between the metal atoms in the same and adjacent layers (3.5 and 4.1 Å).
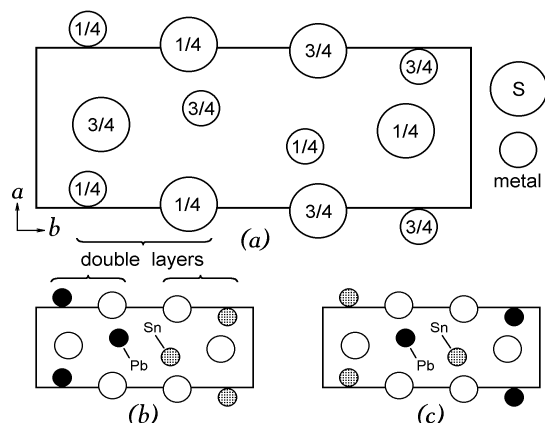


**Figure 4**
Projection of the SnS structure on the *ab*-plane ($a$) and two possible arrangements of the metal atoms in $PbSnS_2$ corresponding to $C_{2v}^7$ ($b$) and $C_{2v}^2$ ($c$) superstructures.

The existence of the short-range order manifests itself in the constitution of the phase diagram of PbS–SnS system. It was already mentioned that the single-phase region of the SnS-based solid solution spreads up to $x \approx 0.5$. According to our data, this composition corresponds to the limiting case, for which the metal atoms are completely ordered in zigzag chains. At higher $x$ the Pb–Pb pairs, the existence of which is energetically unfavorable, would inevitably appear in the chains. So, this simple energy consideration can explain why the composition $x = 0.5$ is the solubility limit of PbS in SnS.

## References

Baak, T., Dietz, E. D., Shouf, M. & Walmsley, J. A. (1966) *J. Chem. and Eng. Data* **11**, 587.

Bigvava, A. D., Kunchuliya, E. D., Moiseenko, S. S. & Anisimov, B. B. (1974) *Izv. AN SSSR, Neorg. mater.* **10**, 359–360.

Chattopadhyay, T., Pannetier, J. & von Schnering, H. G. (1986) *J. Phys. Chem. Solids* **47**, 879–885

von Krebs, H. & Langner, D. (1964) *Z. Anorg. Allg. Chem.* **334**, 37–49.

Kuznetsov, V. G. & Lee Chi-fa (1964) *Zhurn. Neorg. Khimii* **9**, 1201–1206.

Latypov, Z. M., Faizullina N. R., Saveliev, V. N. & Davletshin, R. Yu. (1976) *Izv. AN SSSR, Neorg. mater.* **12**, 206–209.

Lebedev, A. I., Sluchinskaya, I. A., Demin, V. N. & Munro, I. H. (1997) *Phys. Rev. B* **55**, 14770–14773.

Morozov, I. S. & Lee Chi-fa (1963) *Zhurn. Neorg. Khimii* **8**, 1688–1692.

Mustre de Leon, J., Rehr, J. J., Zabinsky, S. I. & Albers R. C. (1991) *Phys. Rev. B* **44**, 4146–4156.

Nuriev, I. R., Salaev, E. Yu. & Nabiev, R. N. (1986) *Izv. AN SSSR, Neorg. mater.* **22**, 204–207.

**Table 1**
Parameters of the local structure of Pb atoms in $Pb_xSn_{1-x}S$.

| $x$ | 0.1 | 0.2 | 0.35 | 0.5 | 0.95 | 1 | SnS[†] |
|---|---|---|---|---|---|---|---|
| $R_1$ | 2.750(8) | 2.745(8) | 2.752(4) | 2.752(4) | 2.954(8) | 2.942(6) | 2.660(3) |
| $\sigma_1^2$ | 0.0066(13) | 0.0053(10) | 0.0087(6) | 0.0079(6) | 0.0095(11) | 0.0086(9) | 0.0036(4) |
| $R_2$ | 3.246(16) | 3.243(16) | 3.233(7) | 3.232(8) | 4.175(7) | 4.184(6) | 3.301(8) |
| $\sigma_2^2$ | 0.0174(35) | 0.0120(26) | 0.0178(14) | 0.0187(16) | 0.0064(7) | 0.0066(6) | 0.0059(8) |
| $R_3$ | 3.534(13) | 3.500(15) | 3.522(7) | 3.535(10) | | | 3.481(7) |
| $\sigma_3^2$ | 0.0081(16) | 0.0090(15) | 0.0118(8) | 0.0141(12) | | | 0.0067(6) |

[†] EXAFS data for the local environment of tin in SnS were obtained at the Sn $K$ edge.